Electronic supplementary information for

Molecular Origin of Structural Defects in the Zinc Phthalocyanine Film

E. G. Odintsova, V. E. Petrenko, A. M. Kolker, N. Yu. Borovkov

G.A. Krestov Institute of Solution Chemistry, Russian Academy of Sciences
Address: 1, Akademicheskaya St., 153045 Ivanovo, Russia
E-mail: phthalocyanine2020@gmail.com

Content

Part 1. DFT Calculations

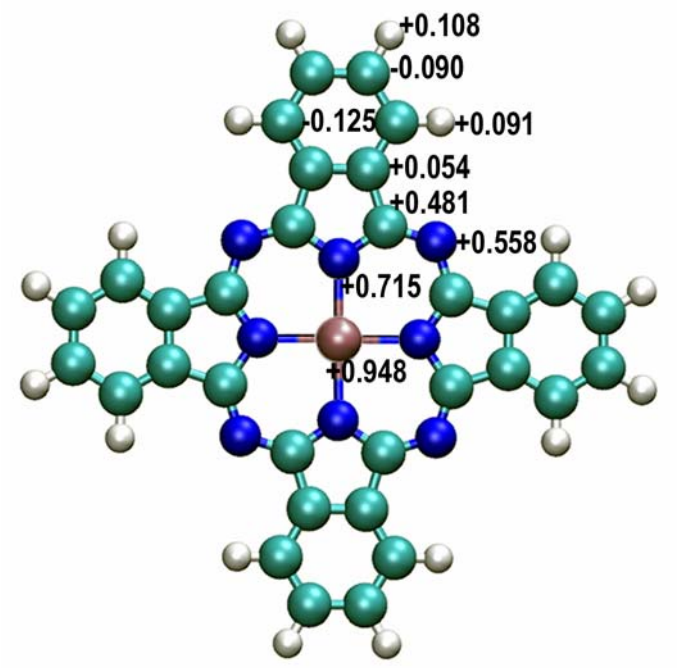

Figure S1. The ZnPc molecule with partial atomic charges inscribed. The atomic charges are obtained by the natural bond orbital (NBO) analysis. The molecular geometry is detailed in **Table S1** below.

Table S1. Bond lengths and angles of the ZnPc molecule.

	**Calculations ***			**Experiments ***	
	A	***B***	***C***	***D***	***E***
Zn-N^1	1.990	1.992	2.002	1.980	1.954
N^1-C^1	1.373	1.373	1.387	1.369	1.374
C^1-N^2	1.330	1.330	1.335	1.331	-
C^1-C^2	1.460	1.461	1.461	1.455	1.420
C^2-C^3	1.395	1.395	1.396	1.393	1.370
C^3-C^4	1.394	1.395	1.399	1.391	1.369
C^2-C^2	1.410	1.410	1.417	1.400	1.550
C^4-C^4	1.407	1.408	1.411	1.396	1.383
C^3-H	1.085	-	1.084	-	-
C^4-H	1.086	-	1.085	-	-
Zn-N^1-C^1	125.3	-	125.4	-	-
N^1-C^1-N^2	127.5	-	127.0	-	-
C^1-N^2-C^1	124.4	124.4	-	123.5	125.6
C^1-N^1-C^1	109.4	109.5	109.1	109.1	106.9
C^2-C^1-N^1	108.8	108.7	108.7	108.8	113.0
C^2-C^2-C^1	106.5	106.5	106.8	106.6	103.5
C^2-C^2-C^3	121.1	-	121.0	-	-
C^2-C^3-C^4	117.8	117.8	117.9	117.3	121.6
C^3-C^4-C^4	121.2	121.2	121.1	121.5	-

* ***A***, DFT-B3LYP/6-31G(d,p), ours; ***B***, DFT-B3LYP/6-31G(d), ref †; ***C***, DFT-B3LYP/6-31G, ref ‡; ***D***, X-ray diffraction, ref †; ***E***, electron diffraction in the gaseous phase, ref †.

† L. T. Ueno et al., Theoretical Studies of Zinc Phthalocyanine Monomer... *J. Mol. Struct. (Theo-chem)* **2009**, *899*, 71; https://doi.org/10.1016/j.theochem.2008.12.013.

‡ G. S. S. Saini et al., Zinc Phthalocyanine Thin Film and Chemical Analyte Interaction... *J. Phys. (Condens. Matter)* **2009**, *21*, 225006; https://doi.org/10.1088/0953-8984/21/22/225006.

Part 2. Molecular Arrangements in the 3D Film

/simulated by dosing 292 molecules into the simulation box/

The structural simulation has been preceded by estimating the binding energy in the 1st monolayer of the ZnPc molecules on the Ag(111) surface.

When the MD method is applied to simulate a molecular system, this energy is determined by using the potential of mean force (PMF), that is, the function whose gradient gives the force between two particles averaged over the equilibrium distribution of all other particles.

Herein PFM has been extracted from the radial distribution function (RDF) calculated along the shortened trajectory of 28 ns:

$$W(r) = -k_B T \cdot \ln[g(r)]$$

where r is the interatomic Zn–Ag distance, g(r) is RDF (the full-trajectory RDF version is shown in **Figure S12**).

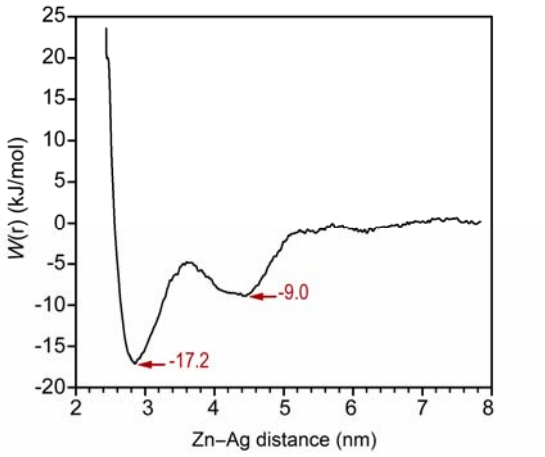

Figure S2. The potential of mean force for the ZnPc–Ag(111) system.

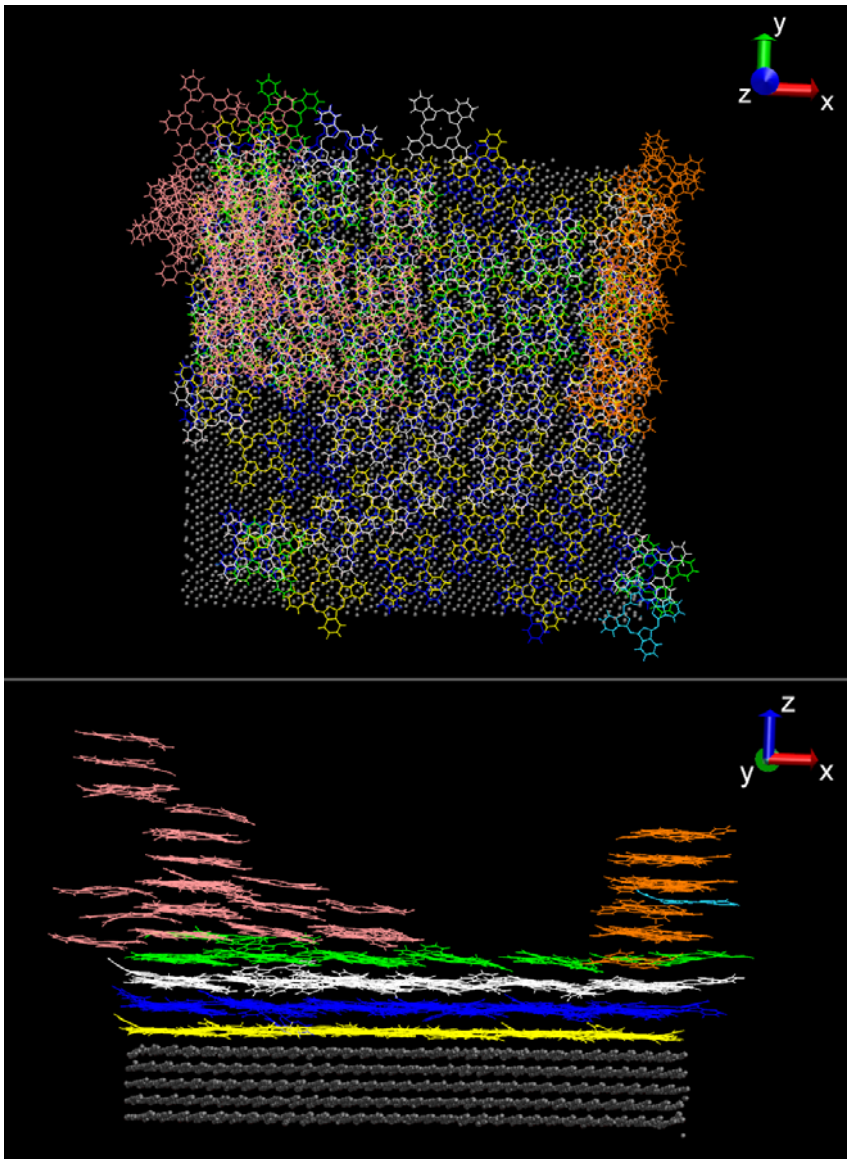

Figure S3. Final snapshots of the ZnPc film. Color code: grey, Ag; yellow, 1st monolayer; blue, 2nd monolayer; white, 3rd monolayer; green, extra layer; rose, tapered island; orange, flat island; cyan; orphan molecules.

Note: The individual layers are analyzed in **Figures S4**–**S8**.

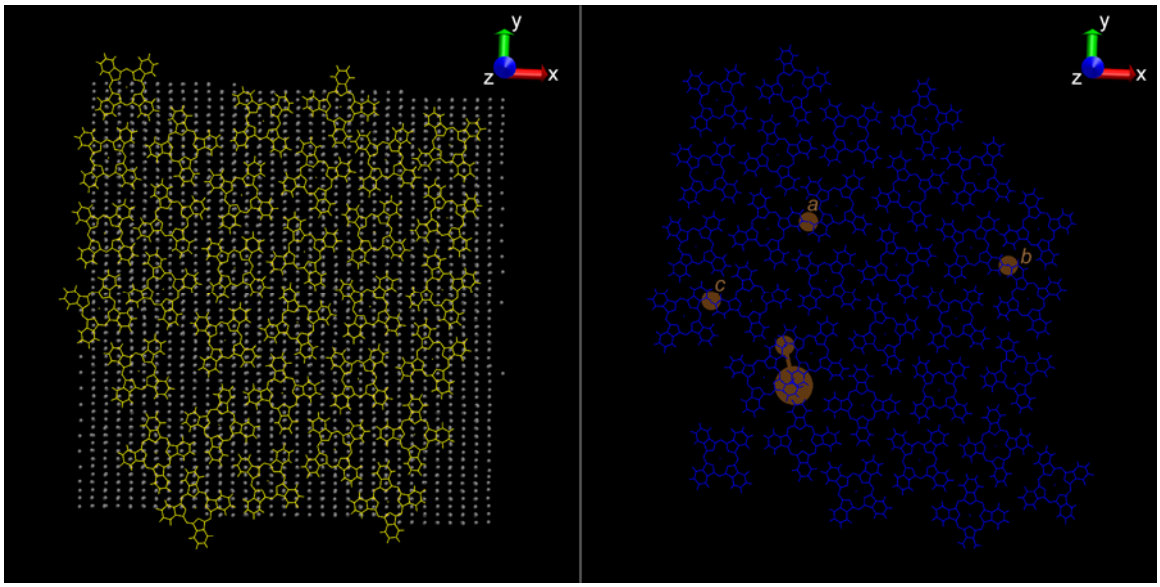

Figure S4. Final snapshots of the individual lower layers. Left: 1st (against Ag). Right: 2nd. Morphological defects are highlighted with brown color. The coarse defect is detailed in **Figures S5** and **S6**; the small defects (*a*–*c*) are described in **Table S2**.

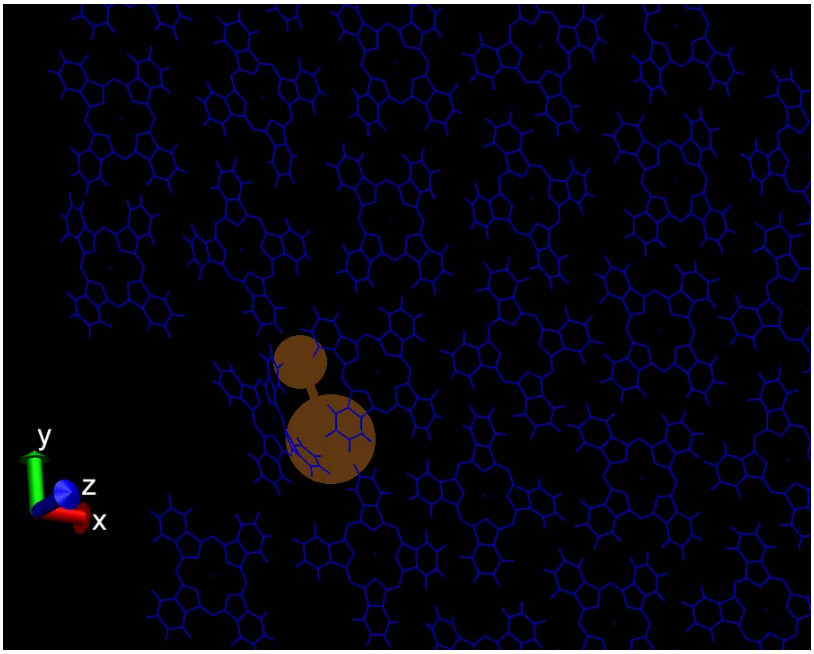

Figure S5. A perspective view of the 2nd layer. Highlighted is the coarse defect caused by steep molecular tilting.

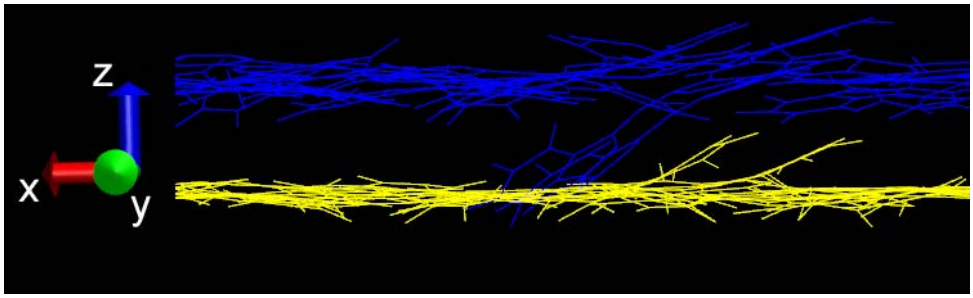

Figure S6. A close-up image of the coarse defect (**Figure S5**).

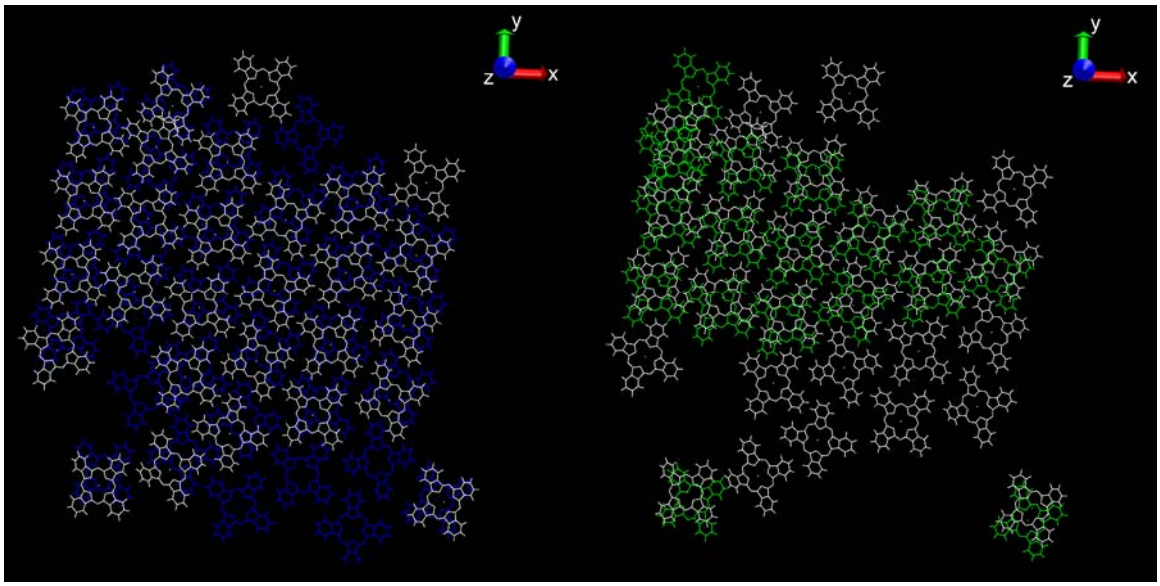

Figure S7. Final snapshots of the superimposed upper layers: Left: 3rd (against 2nd). Right: extra (against 3rd).

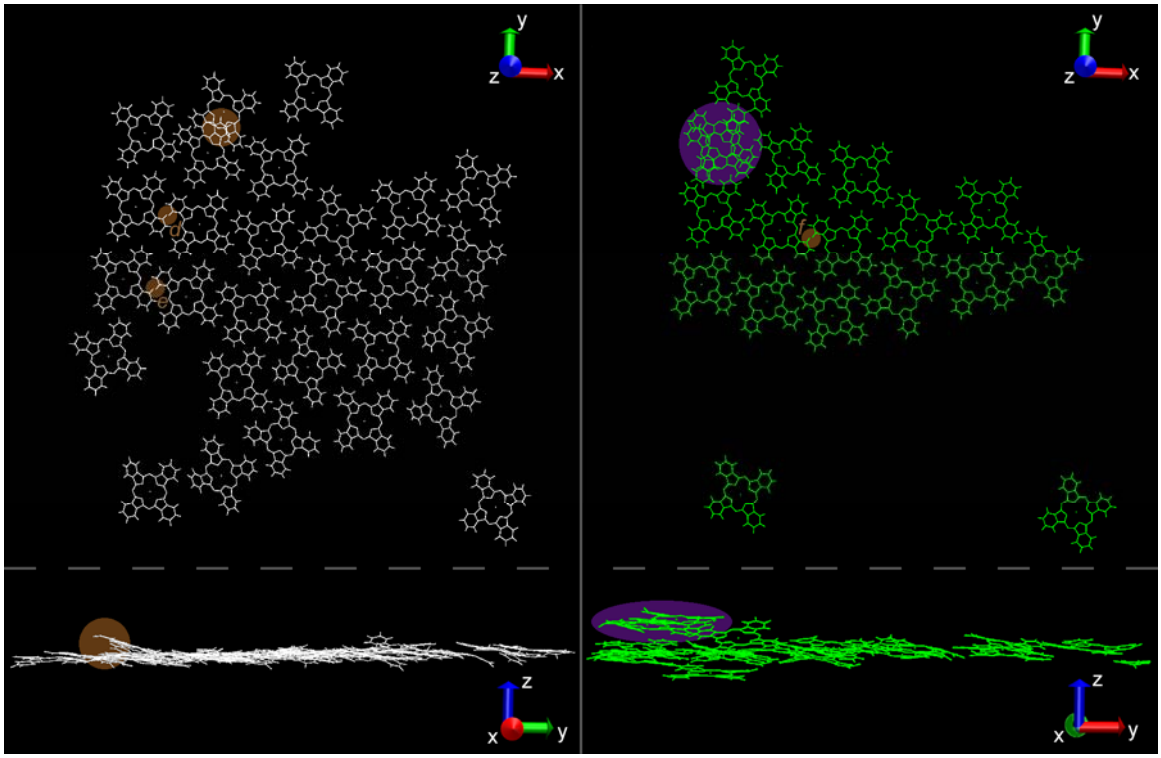

Figure S8. Analysis of two upper layers (**Figure S7, right**). Left: 3rd. Right: extra. Morphological defects are highlighted with brown color. The small defects (*d*–*f*) are described in **Table S2**. Highlighted with violet color is a dimer.

Table S2. Spatial Description of the Small Defects (*a*–*f*) in **Figures S4** and **S8**.

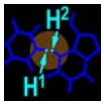	***a***	***b***	***c***	***d***	***e***	***f***
$\mathbf{X_1}$	27.23	67.66	8.81	13.49	11.46	26.54
$\mathbf{X_2}$	28.29	67.09	9.69	14.69	12.57	27.70
$\mathbf{Y_1}$	54.53	48.25	38.98	59.26	45.23	54.21
$\mathbf{Y_2}$	54.62	47.97	38.78	59.14	45.21	54.32
$\mathbf{Z_1}$	20.50	21.09	20.68	23.94	24.39	28.13
$\mathbf{Z_2}$	22.75	23.18	23.62	26.35	26.14	30.20
R	2.49	2.18	3.08	2.65	2.07	2.37

Abbreviations: X_i, Y_i and Z_i, Cartesian coordinates of the H^1 and H^2 atoms (nm); *R*, the spatial H^1–H^2 distance (Å).

Part 3. Structural Features of the 3D Film

/simulated by dosing 292 molecules into the simulation box/

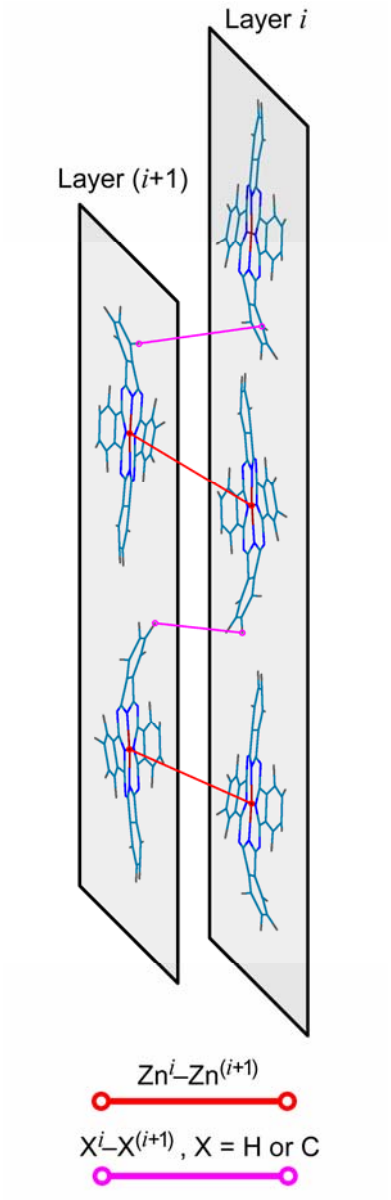

Figure S9. Minimal distances between ZnPc molecules in contiguous layers (depicted vertically for convenience).

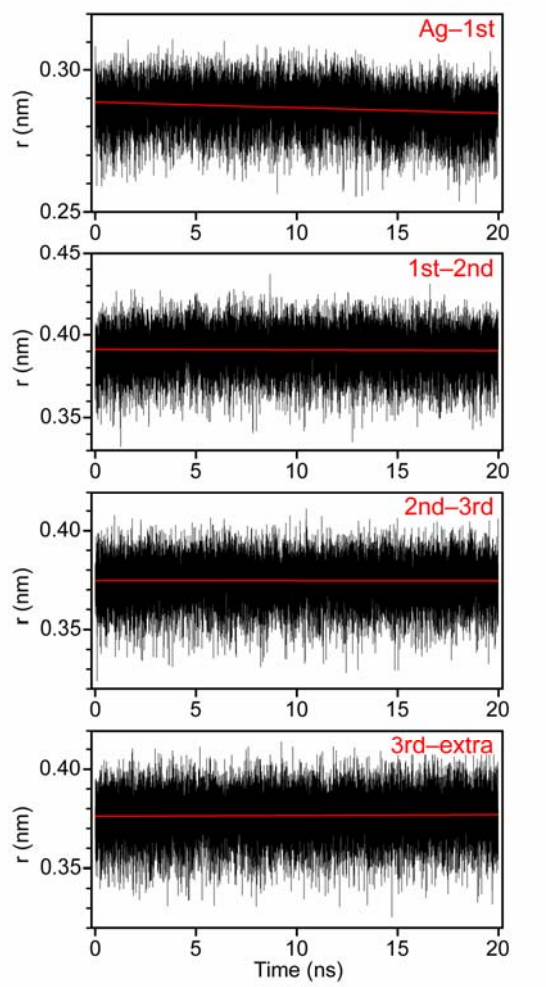

Figure S10. Time evolution of the minimal distances between the Ag substrate, the monolayers (1–3) and the extra layer. The black traces show the minimal distances between metal atoms (Ag–Zn or Zn–Zn) after last 54 molecules have been dosed into the simulation box. The red lines are obtained by linear fitting of the data points.

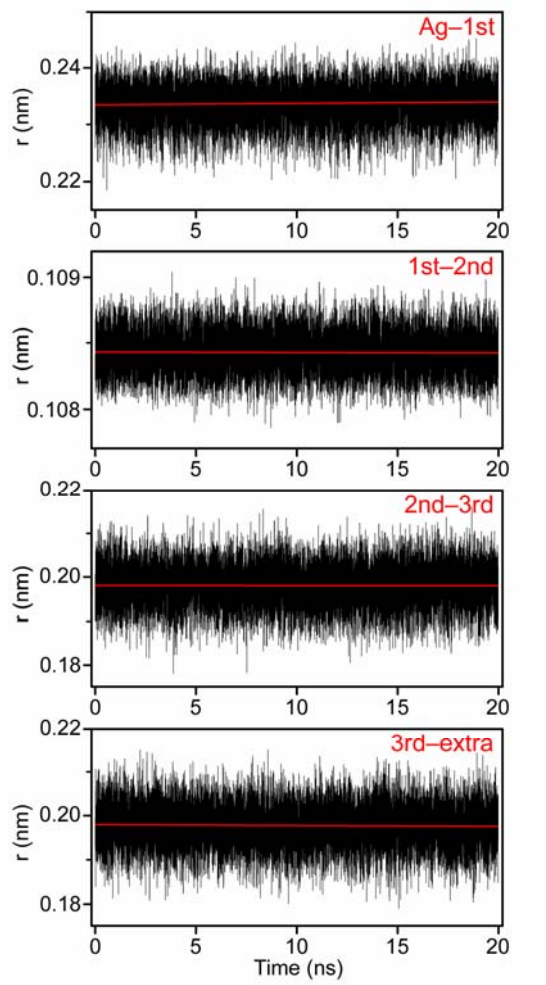

Figure S11. Time evolution of the minimal distances between the Ag substrate, the monolayers (1–3) and the extra layer. The black traces show the clearances (Ag–X or X–X, where X = C or H) after last 54 molecules have been dosed into the simulation box. The red lines are obtained by linear fitting of the data points.

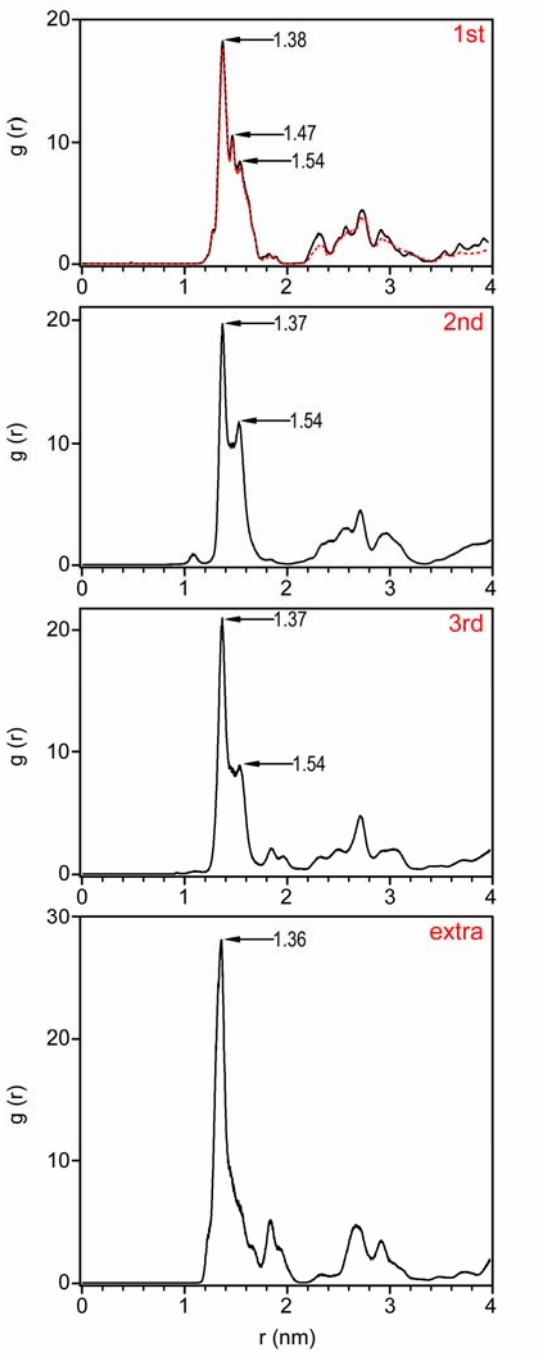

Figure S12. RDF's between Zn atoms within the individual layers (**Figure S3**). All Y-axes are equally scaled.

Note: The top image allows one to compare the 1st monolayer on two kinds of the Ag (111) substrate: black, fully frozen Ag atoms; red, unfrozen topmost surface Ag atoms.

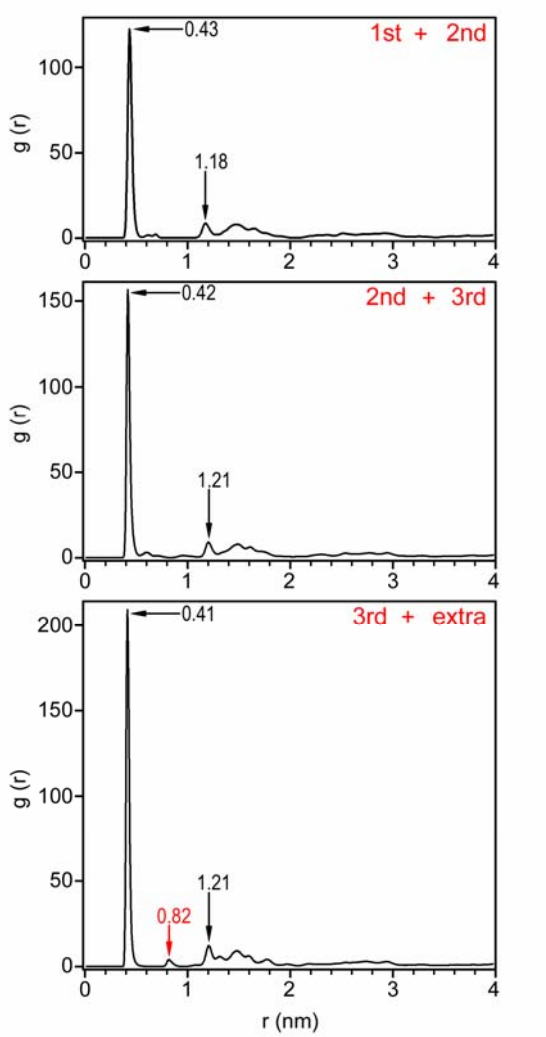

Figure S13. RDF's between Zn atoms located in the contiguous layers (**Figure S3**). All Y-axes are equally scaled. A peak indicated with a red arrow is connected with the 2D→3D transformation.

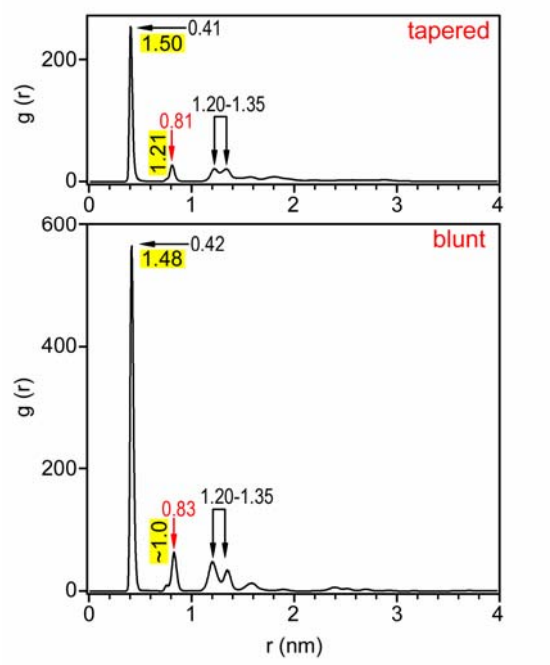

Figure S14. RDF's between Zn atoms located in the islands (**Figure S3**). All Y-axes are equally scaled. Two peaks indicated with red arrows are connected with the 2D→3D transformation. Highlighted with yellow color are coordination numbers.

Note: Coordination number is determined from the equation:

$$N = 4\pi\rho \cdot \int r^2 g(r) dr$$

where ρ is the number density calculated as a ratio of 292 to the cell volume, (8.039 × 8.000 × 8.657) nm^3.

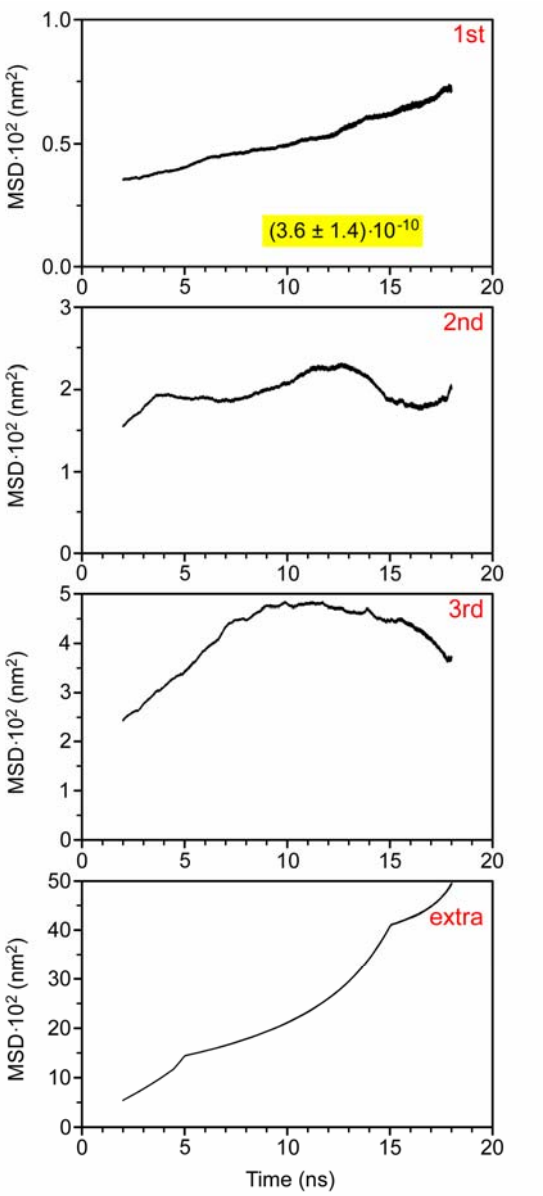

Figure S15. Mean-squared displacements (MSD) vs time plots for the ZnPc molecules in the individual layers (**Figure S3**). Highlighted with yellow color is the diffusion coefficient (D, $cm^2\ s^{-1}$) roughly estimated by linear fitting the data points from 2 ns to 18 ns.

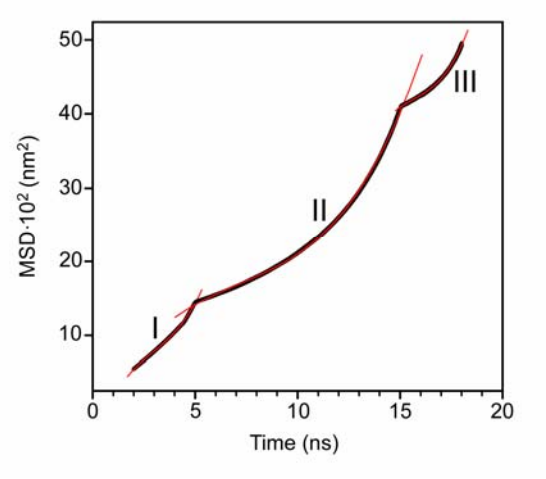

Figure S16. Analysis of the MSD–time plot for the extra layer (**Figure S15, bottom**). The data points (appearing as a black line) are divided into three parts (I, II, III) and fitted with the cubic polynomial (red lines, **Table S3**).

Table S3. Polynomial regression of the MSD–time plot for **Figure S16**.

Part	**Equation Y = A + BX + CX^2 + DX^3**				***r***
	A	**B**	**C**	**D**	
I	-4.287 ± 0.090	7.640 ± 0.082	-1.836 ± 0.024	0.2104 ± 0.0023	0.9993
II	-1.448 ± 0.073	5.372 ± 0.024	-0.5932 ± 0.0025	0.02804 ± 0.00008	0.9995
III	-1027.5 ± 10.8	202.3 ± 2.0	-12.85 ± 0.12	0.2743 ±0.0024	0.9992

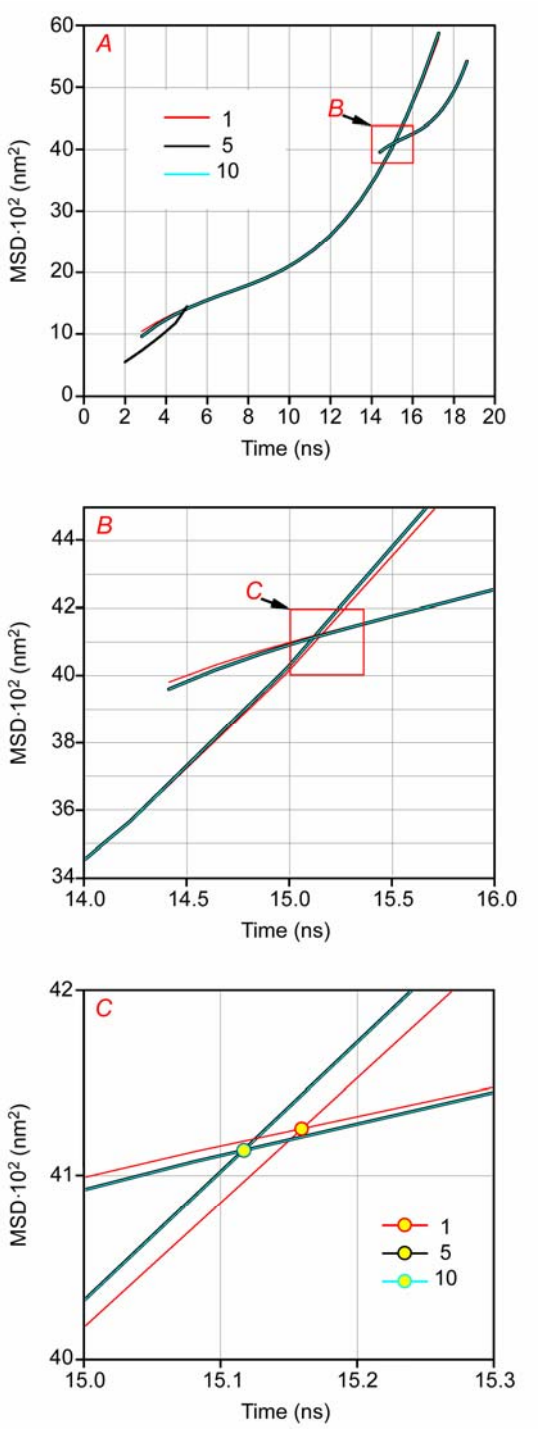

Figure S17. The MSD–time plot (**Figure S16**) illustrating how the number of simulations affects the data point fitting. Top: General view (*A*). Middle: Vicinity of the 2nd potential well (*B*). Bottom: Close view of the potential well (*C*).

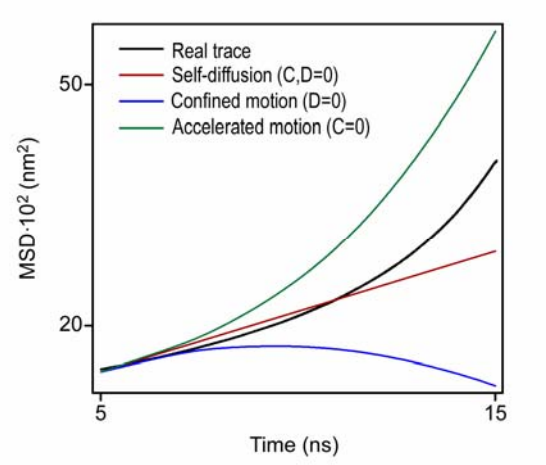

Figure S18. Illustration of the real and theoretical modes of molecular motion for Part II in **Table S3**.

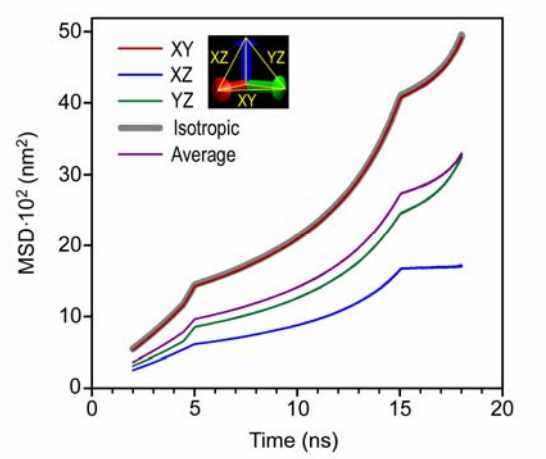

Figure S19. Anisotropic mean-squared displacements (MSD) vs time plots for the ZnPc molecules in the extra layer (**Figure S3**). The grey line is broadened for convenience.

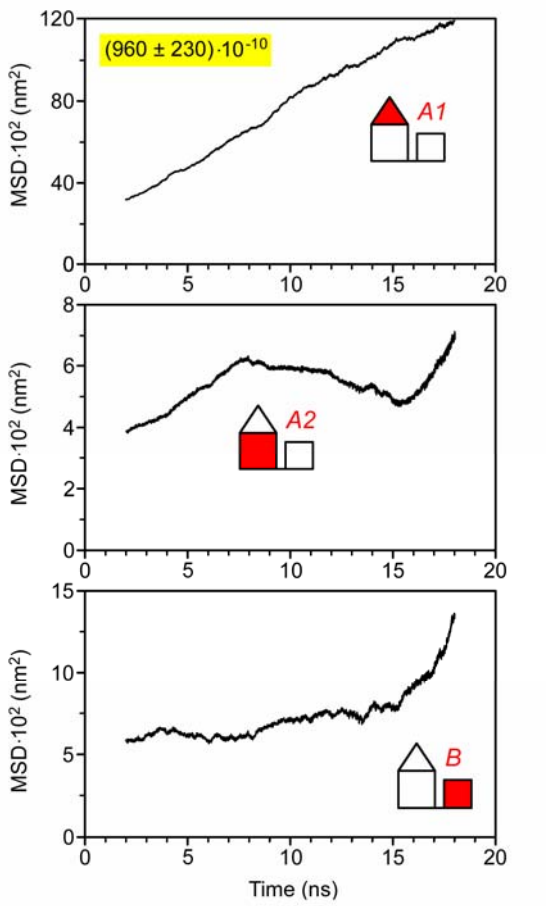

Figure S20. MSD–time plots for the ZnPc molecules located in the islands (**Figure S3**). Pictographs: *A1*, a summit of the tapered island; *A2*, a base of the tapered island; *B*, a whole of the flat island. Highlighted with yellow color is the diffusion coefficients (D, $cm^2\ s^{-1}$) roughly estimated by linear fitting the data points from 2 ns to 18 ns.

Part 4. Molecular Arrangements and Structural Features of the Low-Dimensional Film

/simulated by dosing 238 molecules into the simulation box/

The morphological evolution has been studied on two earlier stages of the film growth. **Part 3** reports on the film, in which the 3D islands are just germinating.

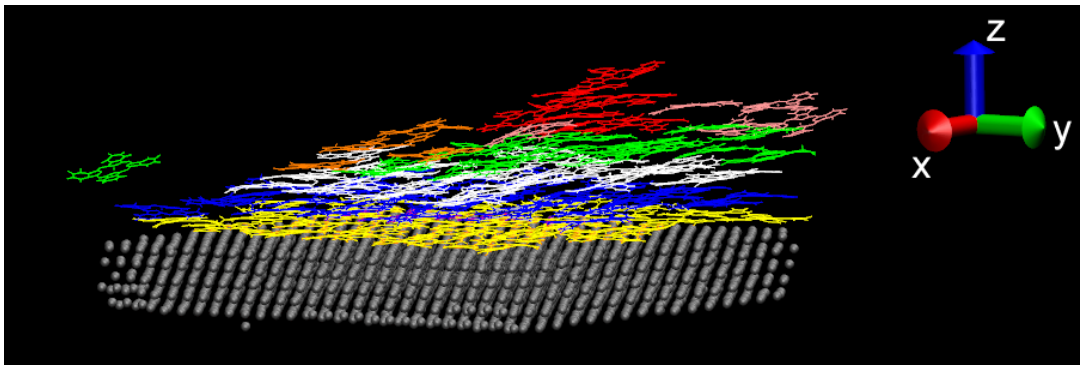

Figure S21. A final snapshot of the ZnPc film (238 molecules). Color code is nearly as in **Figure S3** except for the tapered island depicted here with two colors: rose, loosely packed bilayer; red; compact nucleus.

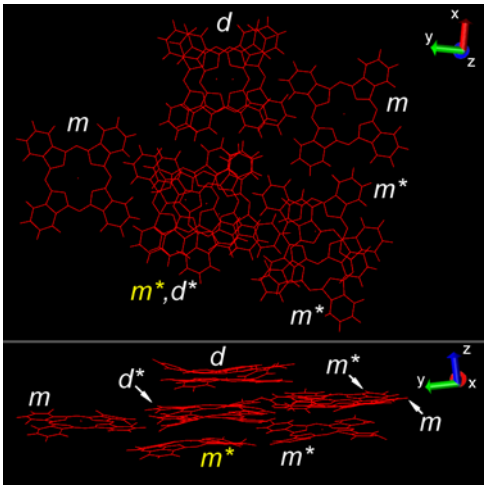

Figure 22. Close-up views of the nucleus (**Figure S21**). Abbreviations: *d*, dimer; *m*, individual molecule. Abbreviations: *m*, molecule; *d*, dimer. All associated entities are marked with asterisk; the domed molecule (**Figure S23**) is marked with a yellow letter.

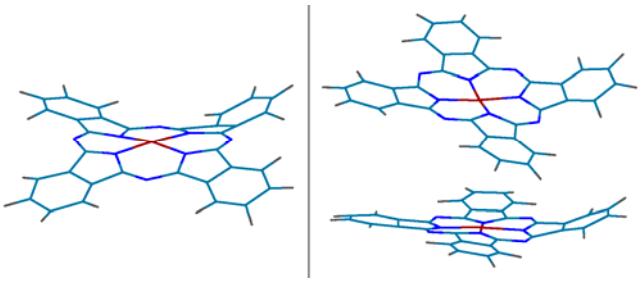

Figure S23. Distortion modes of the ZnPc molecules. Left: ruffled. Right: domed-plus-ruffled. The former mode occurs in the layers and islands; the latter one is found only in the nucleus (**Figure S22**).

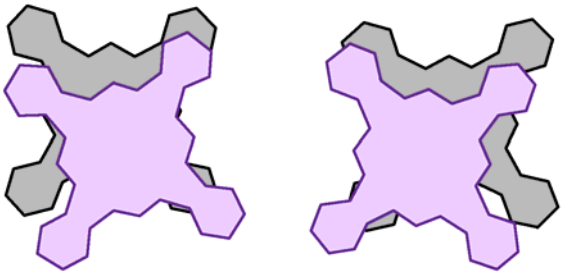

Figure S24. Front projections of two dimers in the nucleus (**Figure S22**).

Part 5. Visualization of the Solution-Deposited ZnPc Films

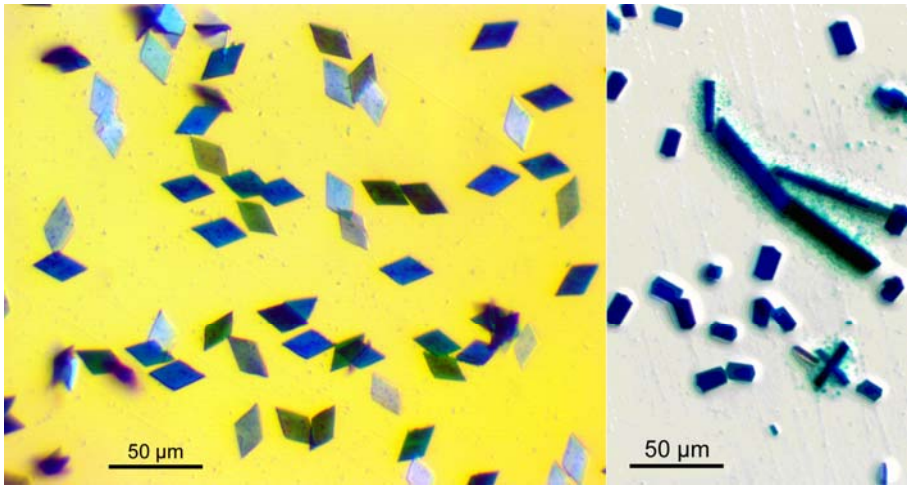

Figure S25. Left: Rhomboid ZnPc crystallites modified with 3-bromopyridine. Right: Non-modified prismatic crystallites for comparison. The both samples are deposited from solution in the binary cyclopentanone–3-dimethylamino-1-propanol system. The images are shown as taken with an Altami Polar 312 microscope and the Altami 14 mega-pixel digital camera USB 2.0 UCMOS14000KPA. (https://altami.ru/cameras/usb2/ucmos/digital_eyepice_ucmos14000kpa/).

Note: The left background looks yellow owing to light scattering from the thicker wetting layer. The rhomboid crystallites appear diversely colored because of different thicknesses.

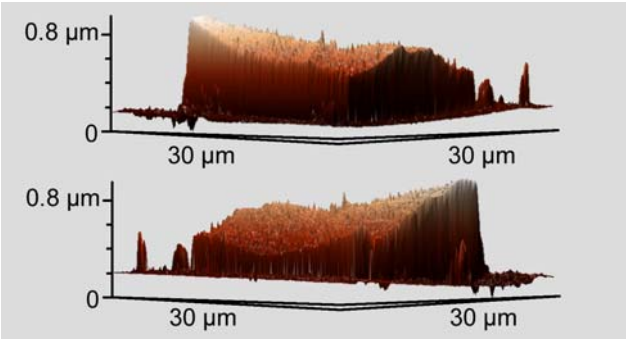

Figure S26. AFM height images of a rhomboid crystallite (side views). Top: Two side planes faced toward the receding crystallization front. Bottom: Two other planes faced away from the crystallization front. The images allow estimating the wetting layer thickness as > 200 nm.

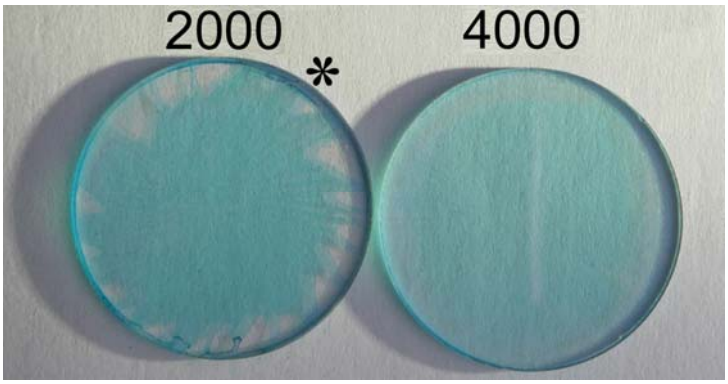

Figure S27. Spin-cast films of ZnPc prepared at two different rotation speeds (rpm). The film with predetermined nonuniformity is marked. The glass slide diameter is 1 inch.

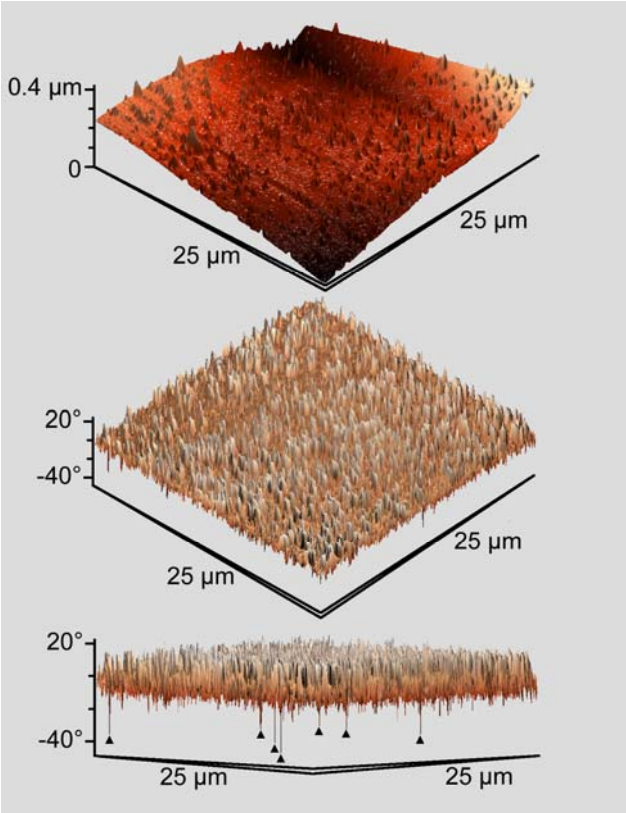

Figure S28. AFM height and phase contrast images of the film marked in **Figure S27**. The images are taken within the central zone (ca. 3/8 inch in diameter). Perspective views (top and middle) demonstrate the congruence between the height and phase contrast images. A side view (bottom) allows one to find out the surface density of dot-like defects (▲).